



Circular RNA circ_0102049 promotes cell progression as ceRNA to target MDM2 via sponging miR-1304-5p in osteosarcoma

Yan Jin^a, Lisen Li^b, Tongtong Zhu^c, Guangyao Liu^{c,*}

^a Department of Ophthalmology, Second Hospital of Jilin University, Changchun, 130000, China

^b Department of Hand Surgery, China-Japan Friendship Hospital of Jilin University, Changchun, 130000, China

^c Department of Orthopedics, China-Japan Friendship Hospital of Jilin University, Changchun, 130000, China

ARTICLE INFO

Keywords:

Osteosarcoma
Circular RNA
Circ_0102049
miR-1304-5p
MDM2

ABSTRACT

Osteosarcoma (OS) is known as a tumor that derives from skeletal system with increasing incidence worldwide. This study aimed to explore the effect of a circular RNA (circRNA), circ_0102049, on OS and reveal its potential molecular mechanism. In this work, the expression of circ_0102049 was detected by quantitative real time polymerase chain reaction (qRT-PCR) in both OS specimens and cell lines. The relationship between circ_0102049 level and patients' overall survival was evaluated by Kaplan-Meier curves and Cox regression analysis. Cell proliferation, apoptosis, migration and invasion of U2OS and MG63 cells were measured by cell counting kit-8 (CCK-8), flow cytometry, wound healing and transwell experiments, respectively. In addition, subcellular fractionation, bioinformatics analysis and dual-luciferase reporter assay were utilized to reveal the mechanism of circ_0102049 in OS. Circ_0102049 was overexpressed in both OS specimens and cells. Moreover, the level of circ_0102049 in OS patients was markedly correlated with larger tumor size, pulmonary metastasis and poor prognosis. Circ_0102049 remarkably accelerated cell proliferation, migration and invasion but attenuated cell apoptosis in OS cells analyzed by gain/loss of function experiments. What's more, we identified that circ_0102049 functions as a competing endogenous RNA (ceRNA) to competitively sponge miR-1304-5p to upregulate MDM2 expression at posttranscriptional level, thus mediating the cellular behaviors of OS cells. Collectively, our study provides an innovatively regulatory mechanism of circ_0102049 in OS and points out a new way for OS treatment.

1. Introduction

Osteosarcoma (OS), the most frequent primary malignant cancer in human skeletal system with increasing incidence worldwide [1]. OS can be treated by the maximal safe surgery accompanied with radiation therapy and chemotherapy [2,3]. However, it is typically associated with a dismal prognosis and poor quality of life owing to its aggressive oncogenesis and recurrence, calling for the urgency of new effective therapeutic strategies.

The field of cancer research has witnessed the great impact of long non-coding RNAs on cancer progression in the past few decades [4]. Moreover, researchers have found that circular RNAs (circRNAs) should also win a place in carcinoma pathology [5,6]. CircRNAs are discovered more than forty years ago and were regarded as useless byproducts at first [7]. They generate from back splicing of protein coding genes and possess a solid circular structure [5]. Recently, the important functions of circRNAs in cancer development have been confirmed [8,9]. For

example, circ-PVT1 can be regarded as a biomarker in gastric cancer and accelerates tumor progression [10]. CircRNAs can directly sponge miRNAs to execute their biological behaviors [11]. For instance, Liu et al. uncovered that ciRS-7 facilitates the growth and metastasis of pancreatic cancer through miR-7-induced EGFR/STAT3 axis activation [12].

Currently, several studies also described the role of a few circRNAs in OS. For example, circ_0007534 is a prognostic marker and accelerates OS cell growth by inhibiting cell apoptosis [13]. Hsa_circ_0002052 inhibits OS biological behaviors via attenuating Wnt/ β -catenin pathway through regulating miR-1205/APC2 axis [14]. Circ-LRP6 facilitates the development of OS via negatively regulating KLF2 and APC expression [15]. However, more effective circRNAs that participate in OS pathogenesis and progression need to be recognized to maximize therapeutic effectiveness. Previously, Liu et al. revealed that circ_0102049 is elevated in OS analyzed by high-throughput sequencing technology [16]. Circ_0102049 is mapped to chr14: 51079976-

* Corresponding author.

E-mail address: exhaojia@sina.com (G. Liu).

51081229 and derived from ATL1 gene locus. Circ_0102049 is 232 bp in length and has not been studied yet. Our findings in this study unveiled a tumor-promoting network of circ_0102049/miR-1304-5p/MDM2 axis in OS, providing a promising effective target for future treatment of OS.

2. Materials and methods

2.1. Sample collection of OS tissues

Seventy-six OS specimens and paired nontumor samples were acquired from our hospital. The tissues were stored in the tubes supplemented with the RNA-later preservative, and well-maintained in liquid nitrogen. Patients where all the tissues derived from were informed and permitted with a written consent and none of these enrolled patients received any treatment prior to this. With approval from the Ethics committee of our hospital, the current study was conducted.

2.2. Cell culture and transfection

Required OS cells (MG63, HOS, Saos2, and U2OS) and corresponding normal cells (hFOB1.19) acquired from the American Type Culture Collection (ATCC; Manassas, VA) were recommended to cultivated in DMEM (Invitrogen, USA) in moist air with 5% CO₂ at 37 °C. 10% fetal bovine serum (10% FBS, Gibco) was also supplied in the media.

To silence circ_0102049, miR-1304-5p, and MDM2 expression, si-circ_0102049-1/-2, miR-1304-5p inhibitor and si-MDM2 specifically targeting circ_0102049, miR-1304-5p and MDM2 together with their respective controls were adopted and commercially purchased from GenePharma (Shanghai, China). A pcDNA 3.1 circRNA mini vector and pcDNA 3.1 vector were applied to ectopic express circ_0102049 and MDM2, respectively. MiR-1304-5p mimics and its negative control (mimics-NC) were also acquired from GenePharma. Transfection of these siRNAs/vectors/miRNA mimics/inhibitor into OS cells was implemented following the instruction of Lipofectamine 3000 (Invitrogen, USA). The siRNA specifically targeting to the spliced junction site of circ_0102049 are shown below: si-circ_0102049-1, 5'-GAAAGAGTCTGATATTTCTTG -3'; si-circ_0102049-2: 5'-TGGAAAATTGAAAGAGTC TGA -3'.

2.3. RNA extraction and quantification

Total RNAs in OS cells were acquired using TRIzol (Invitrogen). High Capacity cDNA Reverse Transcription Kit (ThermoFisher, USA) was utilized to reversely transcribe RNAs into cDNAs. Quantitative real time polymerase chain reaction (qRT-PCR) was conducted by using the Applied Biosystems 7500 Sequence Detection system. Relative expressions were calculated using 2^{-ΔΔCt} method. All data were normalized to GAPDH or U6. The primers are displayed below: circ_0102049, Forward, 5'-CTGCTACCTCATCTGGCTT -3'; Reverse, 5'-AGACCTTGAGGCGTTTTTCCA -3'. MDM2, Forward, 5'-GGGAGATATGTTGTGAAAGAAGC -3'; and Reverse, 5'-CCCTGCCTGATACACAGTAACTT -3'. GAPDH, Forward, 5'-GGGAGCCAAAAGGGTCAT -3'; Reverse, 5'-GAGTCCTTCCACGATACCAA -3'. miR-1304-5p, RT Primer, 5'-GTCGTATCAGTGCAGGGTCCGAGGTATTCGCACTGGATACGACAAACTC -3'; Forward, 5'-GCGGGTGTAGAGTGACATCG -3'; and Reverse, 5'-AGTGCAGGGTCCGAGGTATT -3'. U6, RT primer, 5'-CGCTTCACGAATTTGCGTGTGCAT -3'; Forward, 5'-GCTTCGGCAGCA CATATACTAAAAT -3'; Reverse, 5'-CGCTTCACGAATTTGCGT GTCAT -3'.

2.4. Cell viability detection

With regard to assessing cell viability, cell counting kit-8 (CCK-8) kit (Dojindo, Japan) was employed as instructed. First of all, approximately 2000 cells in triplicate were plated into 96-well plates. CCK-8

solution (10 μl) was thereafter put into each well and maintained for 2 h with temperature set at 37 °C. Finally, SpectraMax M5 microplate reader (MD, USA) was applied for measuring the OD value at 450 nm.

2.5. Apoptosis assay

The apoptosis of U2OS and MG63 cells was evaluated by Annexin V-FITC apoptosis detection kit (Invitrogen, USA). In brief, the transfected U2OS and MG63 cells were collected and resuspended in the provided binding buffer. Afterwards, the transfected cells were dyed using Annexin V-FITC and propidium iodide in a dark room. Subsequently, the apoptotic cells were observed using a flow cytometer (BD Biosciences).

2.6. Wound healing assay

Using a marker pen to draw a horizontal line on the back of 6-well dishes. The method of transfecting cells is the same as before. After washing three times with PBS, adding the medium, the cells were cultured in the incubator. Take pictures at 0 and 36 h after wound created.

2.7. Transwell assay

24-well chambers with 8 μm pore size (Corning, NY, USA) were used for transwell invasion assay in terms of cell invasion detection. The cells (with 1 × 10⁵ cells in each well filled with serum-free media) were seeded in the top compartment which is coated with matrigel (BD, Franklin Lakes, USA) in advance, the bottom compartment was added with medium which is 10% FBS-containing. After a one-day incubation and the removal of cells on the upper chambers, methanol was adopted for fixing lower membrane surface. The cells were dyed by crystal violet. At last, a microscope (Leica, Germany) at 200× magnification was put into use for cell counting.

2.8. Immunoblotting assay

OS cells were lysed with ice-cold RIPA assay buffer. Extracted proteins were separated with SDS-PAGE and then shifted onto PVDF membranes. All membranes were treated with skim milk for 1 h. Proteins were incubated with primary antibodies against MDM2 or GAPDH (Abcam, USA) at 4 °C for 12 h, followed by secondary antibodies incubated at 22–25 °C for 2 h. Protein bands were analyzed with Gel-Doc 200 (Bio-Rad, CA, USA). GAPDH was applied as the internal reference.

2.9. Nuclear/cytoplasmic fractionation

In order to separate cytoplasmic and nuclear RNA in U2OS and MG63 cells, the two fractions including cytoplasm and nuclear of these cells were segmented as directed by the protocols of a PARIS kit (Life Technologies). Following qRT-PCR (SYBR Premix Ex Taq; TaKaRa) estimated the extracted RNAs from the cytoplasmic and nuclear fractions.

2.10. Dual luciferase reporter assay

Wild type or mutant circ_0102049 containing predicted binding site with miR-1304-5p were amplified and cloned into pmirGLO vectors (Promega, Madison, USA). The vectors were labelled as circ_0102049-WT and Circ_0102049-Mut. circ_0102049-WT or circ_0102049-Mut was transfected along with miR-NC or miR-1304-5p mimics with Lipofectamine 3000 into OS cells. Forty-eight hours later, luciferase activities were evaluated using a Dual-Luciferase Reporter Assay System (Promega). Similarly, MDM2 3'-UTR-WT or MDM2 3'-UTR-Mut was co-transfected with NC mimics or miR-1304-5p mimics into OS cells and luciferase activities were detected.

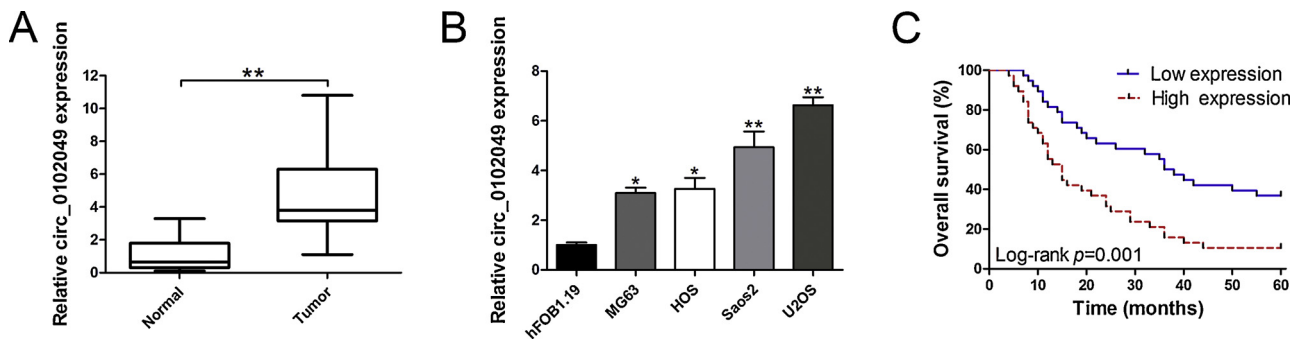


Fig. 1. Relative expression of circ_0102049 in OS tissues and cell lines and its clinical significance. (A) Relative expression of circ_0102049 in OS tissue samples and their paired non-cancerous tissue samples measured by qRT-PCR. (B) Relative expression of circ_0102049 in OS cell lines and hFOB1.19 measured by qRT-PCR. (C) Kaplan-Meier survival analysis was used to assess circ_0102049 expression and OS patients' overall survival. B: The data are shown as the mean \pm SD (n = 3). * $p < 0.05$, ** $p < 0.01$.

2.11. Data analysis

The data were analyzed by GraphPad Prism 5.01 (GraphPad, San Diego, CA, USA) and SPSS 22.0 software (IBM, USA). All data are presented as mean \pm SD. Data were analyzed using Student's *t*-test or one-way analysis of variance between groups. Fisher's exact test was used to analyze the correlation of circ_0102049 and clinical features. Kaplan-Meier analysis with log-rank test and Cox regression were applied to evaluate the prognostic role of circ_0102049. $P < 0.05$ was considered to be statistically significant.

3. Results

3.1. Circ_0102049 is overexpressed in OS tissues and cells and associates with poor prognosis

To unveil the expression profile of circ_0102049 in OS. We firstly explored the level of circ_0102049 in OS specimens and cell lines. The data of qRT-PCR showed that circ_0102049 expression in OS tissues was markedly higher than that in the paracancerous specimens (Fig. 1A). Similarly, circ_0102049 expression was remarkably increased in MG63, HOS, Saos2, and U2OS cells relative to hFOB1.19 cell line (Fig. 1B). Then, the patients were divided into two groups according to the median value of circ_0102049 expression. As Table 1 indicated, high

Table 1
Circ_0102049 expression and clinicopathologic characteristics of osteosarcoma patients.

Clinicopathologic characteristics	No. of patients	Circ_0102049 expression		<i>p</i>
		High	Low	
Gender				0.469
Male	50	27(35.52%)	23(30.26%)	
Female	26	11(14.47%)	15(19.74%)	
Age (years)				0.305
< 30	55	30(39.47%)	25(32.89%)	
\geq 30	21	8(10.53%)	13(17.11%)	
Tumor size (cm)				0.022
< 6	54	22(28.95%)	32(42.11%)	
\geq 6	22	16(21.05%)	6(7.89%)	
WHO grade				0.192
I-II	56	25(32.89%)	31(40.79%)	
III	20	13(17.11%)	7(9.21%)	
Pulmonary metastasis				0.026
Yes	17	13(17.11%)	4(5.26%)	
No	59	25(32.89%)	34(44.74%)	
Differentiation grade				0.100
Well/moderately	46	19(25.00%)	27(35.53%)	
Poorly/undifferentiated	30	19(25.00%)	11(14.47%)	

WHO: World Health Organization.

circ_0102049 expression was associated with larger tumor size ($p = 0.022$) and positive pulmonary metastasis ($p = 0.026$). We also found that the expression of circ_0102049 was remarkably correlated with patients' poor overall survival analyzed by Kaplan-Meier curves (Fig. 1C). Further multivariate analysis demonstrated that larger tumor size ($p = 0.015$), pulmonary metastasis ($p = 0.004$), and elevation of circ_0102049 expression ($p = 0.023$) in tumor tissues were independent factors for OS patients after surgery (Table 2)

3.2. Circ_0102049 promotes the growth, migration and invasion but inhibits the apoptosis of OS cells

We further silence and overexpress the level of circ_0102049 in U2OS and MG63 cells, respectively. The data demonstrated that circ_0102049 expression was strikingly inhibited after transfected with si-circ_0102049-1 or si-circ_0102049-2 compared with si-NC group in U2OS cell line (Fig. 2A). Meanwhile, when compared with empty vector group, circ_0102049 expression of MG63 cells was markedly increased in circ_0102049 vector group (Fig. 2B), suggesting that the transfection was successful. For functional assays, the results of CCK-8 displayed that the cell viability of U2OS cells was markedly decreased in circ_0102049 depletion group compared with si-NC group at 48, 72, and 96 h (Fig. 2C). When compared with empty vector group, the proliferation ability of MG63 cells was remarkably increased in circ_0102049 overexpressed group (Fig. 2C). Furthermore, apoptosis assay also confirmed that silencing of circ_0102049 expression markedly increased the rate of apoptosis in U2OS cells, while circ_0102049 overexpression significantly decreased the number of apoptotic cells (Fig. 2D). To verify the function of circ_0102049 on OS cell migration, wound healing assay was conducted in both U2OS and MG63 cells. As shown in Fig. 2E, silencing of circ_0102049 expression dramatically decreased the wound closure area in U2OS cell line. However, circ_0102049 overexpression significantly promoted wound healing rate in MG63 cells (Fig. 2E). What's more, transwell assay was also carried out to detect cell metastatic properties affected by circ_0102049 in OS cells. As a result, silenced circ_0102049 remarkably decreased U2OS cell migration and invasion (Fig. 2F). By contrast, circ_0102049 overexpression markedly increased cell migratory and invasive potential in MG63 cells (Fig. 2F). The results above suggested that circ_0102049 contributes to OS cell development and progression in vitro.

3.3. Circ_0102049 upregulates MDM2 expression through sponging miR-1304-5p

To uncover the mechanism of circ_0102049 on OS cells, the localization of circ_0102049 in OS cells was analyzed by subcellular fractionation experiment. The data demonstrated that circ_0102049 was

Table 2
Univariate and multivariate analysis of prognostic factors for overall survival in osteosarcoma patients.

Variables	Univariate analysis			Multivariate analysis		
	HR	95% CI	p	HR	95% CI	p
Overall Survival						
Gender (Male vs. Female)	1.181	0.682-2.045	0.552			
Age (≥ 30 vs. < 30)	1.115	0.626-1.985	0.712			
Tumor size (≥ 6 cm vs. < 6 cm)	1.962	1.136-3.389	0.016	2.015	1.143-3.551	0.015
WHO grade (III vs. I-II)	1.494	0.838-2.662	0.173			
Pulmonary metastasis (Yes vs. No)	3.022	1.684-5.424	< 0.001	2.520	1.341-4.733	0.004
Differentiation grade (Poorly/undifferentiated vs. Well/moderately)	2.193	1.302-3.692	0.003	1.497	0.841-2.662	0.170
Circ_0102049 expression (High vs. Low)	2.407	1.415-4.095	0.001	1.929	1.093-3.402	0.023

HR: hazard ratio, 95% CI: 95% confidence interval.

enriched in cytoplasm (Fig. 3A), suggesting that circ_0102049 may regulate downstream targets expression at post-transcriptional level. With the assistance of bioinformatics analysis, we discovered that there were 7 miRNAs potentially binding with circ_0102049. For the sake of further screening, qRT-PCR assay was applied for examination of miRNA expression in OS cells and the results suggested that only miR-1304-5p was upregulated after knockdown of circ_0102049 in U2OS cell line. In MG63 cells, miR-1304-5p was downregulated in the circ_0102049 overexpression group. The levels of the other miRNAs were not influenced by circ_0102049 (Fig. 3B). Moreover, the negative

association between miR-1304-5p and circ_0102049 was also demonstrated by Pearson's correlation analysis (Fig. 3C). Based on these results, miR-1304-5p was chosen as the study subject. Then, the result of luciferase reporter test exposed that elevation of miR-1304-5p only mitigated the luciferase activity of circ_0102049-WT, whereas luciferase activity of circ_0102049-MUT had no response to miR-1304-5p overexpression (Fig. 3D and E). These data proved the interaction of miR-1304-5p with circ_0102049. We further predicted that MDM2 may be the downstream target of miR-1304-5p (Fig. 3F). It was uncovered that ectopic expression of miR-1304-5p inhibited MDM2 expression,

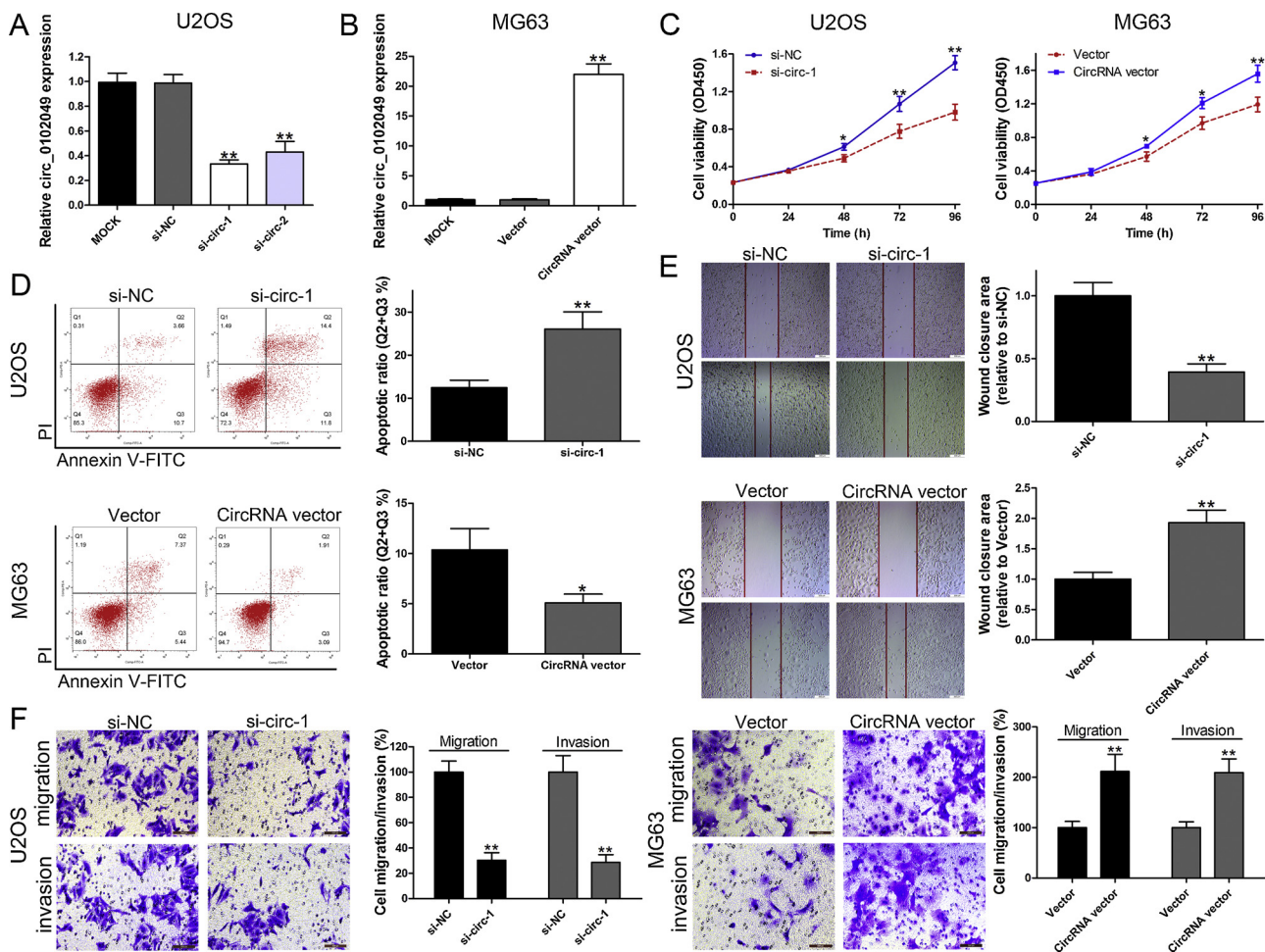


Fig. 2. Circ_0102049 contributes to OS cell progression. (A) Circ_0102049 expression was detected after transfection in U2OS cells by qRT-PCR. (B) Circ_0102049 expression was detected after transfection in MG63 cells by qRT-PCR. (C) CCK-8 assays were used to detect cell viability of U2OS and MG63 cells after transfection. (D) Flow cytometric analysis was used to detect cell apoptosis of U2OS and MG63 cells after transfection. (E) Wound healing assays were used to detect cell migration of U2OS and MG63 cells after transfection. (F) Transwell assays were used to detect cell migration and invasion capacities of U2OS and MG63 cells after transfection. Scale bar = 50 μ m. A-F: The data are shown as the mean \pm SD (n = 3). * p < 0.05, ** p < 0.01.

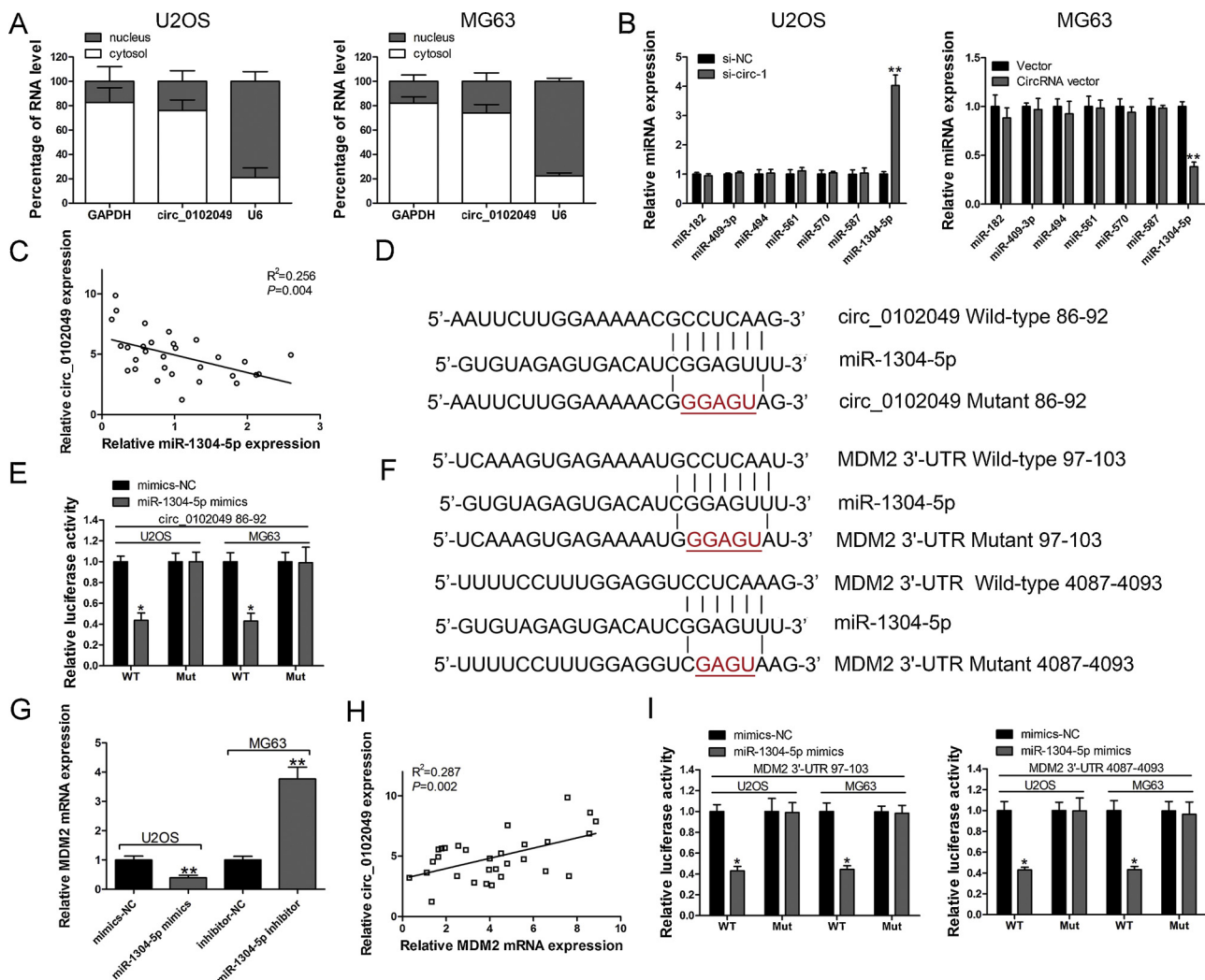


Fig. 3. Circ_0102049 sponges miR-1304-5p to elevate MDM2 expression. (A) qRT-PCR detection of the percentage of circ_0102049, GAPDH and U6 in the cytoplasm and nuclear fractions of U2OS and MG63 cells. GAPDH and U6 were used as cytoplasmic and nuclear localization markers, respectively. (B) Relative miRNA expression was detected in U2OS and MG63 cells after transfection. (C) Correlation analysis of circ_0102049 and miR-1304-5p in OS patients' tissues. (D) Diagrammatic sketch of the binding site for circ_0102049 and miR-1304-5p. (E) Luciferase reporter assay was conducted to evaluate the interaction ability between miR-1304-5p and circ_0102049. (F) Diagrammatic sketch of the binding sites for MDM2 3'-UTR and miR-1304-5p. (G) Relative MDM2 mRNA expression was detected in U2OS and MG63 cells after transfection. (H) Correlation analysis of circ_0102049 and MDM2 mRNA in OS patients' tissues. (I) Luciferase reporter assay was conducted to evaluate the interaction ability between MDM2 3'-UTR and miR-1304-5p. A,B,C,E,G,I: The data are shown as the mean \pm SD ($n = 3$). * $p < 0.05$, ** $p < 0.01$.

while miR-1304-5p inhibitor evidently promoted the level of MDM2 mRNA (Fig. 3G). More importantly, circ_0102049 expression was positively correlated with MDM2 mRNA level (Fig. 3H). Further dual-luciferase reporter assay indicated that both of the two predicted binding sites of miR-1304-5p within MDM2 3'-UTR were functional (Fig. 3I). Collectively, circ_0102049 sponged miR-1304-5p to enhance MDM2 level in OS.

3.4. The oncogenic functions of circ_0102049 are partly attributed to its regulation of MDM2

Subsequently, rescue experiments were performed to verify the role of circ_0102049/miR-1304-5p/MDM2 in OS. Firstly, we proved that the protein expression of MDM2 was decreased by circ_0102049 depletion and then recovered under co-transfection with MDM2 vector in U2OS cell line (Fig. 4A). What's more, MDM2 level was significantly elevated after circ_0102049 overexpression and after co-transfection with si-MDM2, its expression was partly decreased in MG63 cells (Fig. 4A). As displayed in Fig. 4B-D, CCK-8, flow cytometric and transwell assays

unveiled that the malignant biological behaviors were attenuated by inhibition of circ_0102049 and then recovered by cotransfected with MDM2 vector in U2OS cell line (Fig. 4B-D). Conversely, MDM2 knockdown offset the promotion of circ_0102049 vector on cell progression in MG63 cells (Fig. 4B-D). Namely, we concluded that circ_0102049 executed its function in the progression of OS by modulation of MDM2.

4. Discussion

OS, the most common primary bone malignancy, is diagnosed mainly in adolescents all over the world. In developing countries, the survival rate of OS patients is still below 30% [1]. It is urgent to investigate new and effective molecular targets for the treatment of OS. More and more evidence demonstrated that circRNAs play a carcinogenic or anticancer role in various malignant tumors, such as hsa_circ_0007534, hsa_circ_0002052, circ-LRP6 [13–15], etc. In addition, circRNAs are reported to be abnormally expressed in tumors [17]. For example, circ-SCAF11 accelerates glioma cell tumorigenesis through

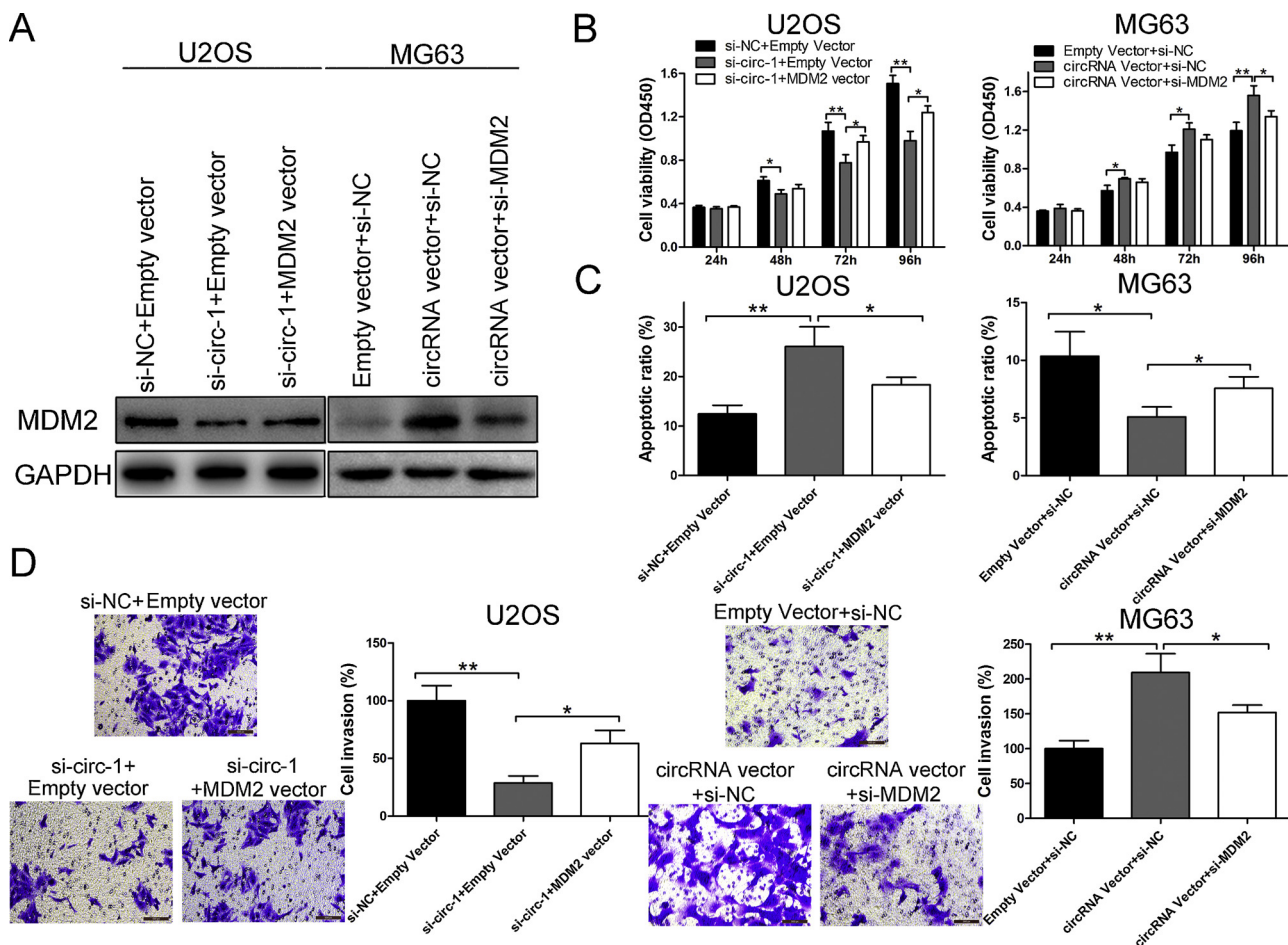


Fig. 4. The oncogenic role of circ_0102049 is dependent on its regulation of MDM2. (A) MDM2 expression was detected in U2OS and MG63 cells after transfection. (B) CCK-8 assay was used to evaluate cell viability after transfection in U2OS and MG63 cells. (C) Flow cytometric assay was used to evaluate cell apoptosis after transfection in U2OS and MG63 cells. (D) Transwell assays were used to evaluate cell invasive potential after transfection in U2OS and MG63 cells. B,C,D: The data are shown as the mean \pm SD ($n = 3$). * $p < 0.05$, ** $p < 0.01$.

the miR-421/SP1/VEGFA axis [18]. Another study demonstrated that circRNA_101505 sensitizes hepatocellular carcinoma cells to cisplatin via sponging miR-103 and enhances oxidored-nitro domain-containing protein 1 expression [19].

For circ_0102049, previous researchers have confirmed that the expression of circ_0102049 is upregulated in OS screened by high-throughput sequencing technology [16]. Circ_0102049 is located at chr14: 51079976-51081229 and derived from ATL1 gene locus. Circ_0102049 is 232 bp in length. The clinical significance, functional role and mechanism of circ_0102049 were not studied before. In this project, we assessed the expression of circ_0102049 in both OS tissues and cells, and identified that circ_0102049 was overexpressed in both OS specimens and cells. Furthermore, we also found circ_0102049 expression was linked to lower overall survival. What's more, gain and loss of function assay uncovered its oncogenic role in OS development and progression. It accelerates OS cell growth by inhibiting cell apoptosis and facilitates cell migratory and invasive potential in vitro. For this part, animal study is still needed to further verify the in vitro results in the future studies.

Accumulating studies have confirmed that circRNAs take in the regulation of cell growth, migration and angiogenesis in various diseases by acting as a competing endogenous RNA (ceRNA) to modulate downstream target expression at posttranscriptional level [20]. For example, Yang et al., reported that circ-ITGA7 sponges miR-3187-3p to elevate ASXL1 expression, thus suppressing colorectal cancer progression [21]. In this project, after confirming the localization of

circ_0102049 in OS cells, bioinformatics analysis (Circular RNA Interactome and TargetScan online databases), qRT-PCR and dual-luciferase reporter assay were applied to investigate the potential mechanisms of circ_0102049. Thus, circ_0102049/miR-1304-5p/MDM2 axis was identified for the first time. MiR-1304-5p has been reported as a tumor suppressor in several human malignancies. It can be sponged by circ_0025033 and represses papillary thyroid cancer cell growth and metastasis [22]. In NSCLC, miR-1304-5p functions as a tumor suppressor and target 3'-UTR of pancreatic progenitor cell differentiation and proliferation factor (PPDPF) and metastasis-associated in colon cancer 1 (MACC1) to regulate their expression levels [23]. MDM2 is an oncoprotein which promotes the rapid degradation of the tumor suppressor p53 [24]. In contrast to other tumor suppressors such as Rb, p16, or PTEN, p53 is frequently overexpressed in tumors, although its function is ablated. Actually, mutant p53 is frequently upregulated in ovarian cancer cells. However, wild-type p53 is diminished in cells. Suppression of the interaction between MDM2 and p53 could stabilize p53 protein, thus leading to suppression of cancer progression [25]. Various studies have indicated its oncogenic function in tumorigenesis, including esophageal squamous cell carcinoma [26], breast cancer [27], lung adenocarcinoma [28], etc. In the present study, rescue assay further identified that the oncogenic properties of circ_0102049 are attributed to its modulation of MDM2. However, some limitations are still existed in this work. More patients are needed to recruit in the study to further reveal the clinical value of circ_0102049. Other potential targets of circ_0102049 was not explored and needs further

revelation. Additionally, animal study is still needed to elucidate the in vitro results in the future study.

Collectively, our work confirmed that circ_0102049 was dramatically elevated in both OS tissues and cells. In addition, we found that circ_0102049 could promote cell growth, migration and invasion, as well as inhibit cell apoptosis via regulating miR-1304-5p/MDM2 axis. Our research provides an innovatively regulatory mechanism about circ_0102049 in OS and points out a new way to OS treatment.

Acknowledgement

Not applicable.

References

- [1] K. Ando, M.F. Heymann, V. Stresing, et al., Current therapeutic strategies and novel approaches in osteosarcoma, *Cancers (Basel)* 5 (2013) 591–616.
- [2] B. Wang, M. Xu, K. Zheng, et al., Effect of unplanned therapy on the prognosis of patients with extremity osteosarcoma, *Sci. Rep.* 6 (2016) 38783.
- [3] M.A. Anwar, C. El-Baba, M.H. Elnaggar, et al., Novel therapeutic strategies for spinal osteosarcomas, *Semin. Cancer Biol.* (2019), <https://doi.org/10.1016/j.semcancer.2019.05.018>.
- [4] Y. Xu, Y. Yao, X. Jiang, et al., SP1-induced upregulation of lncRNA SPRY4-IT1 exerts oncogenic properties by scaffolding EZH2/LSD1/DNMT1 and sponging miR-101-3p in cholangiocarcinoma, *J. Exp. Clin. Cancer Res.* 37 (2018) 81.
- [5] S. Memczak, A. Jens, M. Elefsinioti, et al., Circular RNAs are a large class of animal RNAs with regulatory potency, *Nature* 495 (2013) 331–338.
- [6] Y. Xu, Y. Yao, X. Zhong, et al., Downregulated circular RNA hsa_circ.0001649 regulates proliferation, migration and invasion in cholangiocarcinoma cells, *Biochem. Biophys. Res. Commun.* 496 (2018) 455–461.
- [7] M.T. Hsu, M. Coca-Prados, Electron microscopic evidence for the circular form of RNA in the cytoplasm of eukaryotic cells, *Nature* 280 (1979) 339–340.
- [8] I.L. Patop, S. Kadener, circRNAs in Cancer, *Curr. Opin. Genet. Dev.* 48 (2018) 121–127.
- [9] Y. Xu, Y. Yao, K. Leng, et al., Increased expression of circular RNA circ_0005230 indicates dismal prognosis in breast cancer and regulates cell proliferation and invasion via miR-618/CBX8 signal pathway, *Cell. Physiol. Biochem.* 51 (2018) 1710–1722.
- [10] J. Chen, Y. Li, Q. Zheng, et al., Circular RNA profile identifies circPVT1 as a proliferative factor and prognostic marker in gastric cancer, *Cancer Lett.* 388 (2017) 208–219.
- [11] T.B. Hansen, T.I. Jensen, B.H. Clausen, et al., Natural RNA circles function as efficient microRNA sponges, *Nature* 495 (2013) 384–388.
- [12] L. Liu, F.B. Liu, M. Huang, et al., Circular RNA ciRS-7 promotes the proliferation and metastasis of pancreatic cancer by regulating miR-7-mediated EGFR/STAT3 signaling pathway, *Hepatobiliary Pancreat. Dis. Int.* (2019), <https://doi.org/10.1016/j.hbpd.2019.03.003>.
- [13] B. Li, X. Li, Overexpression of hsa_circ_0007534 predicts unfavorable prognosis for osteosarcoma and regulates cell growth and apoptosis by affecting AKT/GSK-3 β signaling pathway, *Biomed. Pharmacother.* 107 (2018) 860–866.
- [14] Z. Wu, W. Shi, C. Jiang, Overexpressing circular RNA hsa_circ.0002052 impairs osteosarcoma progression via inhibiting Wnt/ β -catenin pathway by regulating miR-1205/APC2 axis, *Biochem. Biophys. Res. Commun.* 502 (2018) 465–471.
- [15] S. Zheng, Z. Qian, F. Jiang, et al., CircRNA LRP6 promotes the development of osteosarcoma via negatively regulating KLF2 and APC levels, *Am. J. Transl. Res.* 11 (2019) 4126–4138.
- [16] W. Liu, J. Zhang, C. Zou, et al., Microarray expression profile and functional analysis of circular RNAs in osteosarcoma, *Cell. Physiol. Biochem.* 43 (2017) 969–985.
- [17] J. Li, J. Yang, P. Zhou, et al., Circular RNAs in cancer: novel insights into origins, properties, functions and implications, *Am. J. Cancer Res.* 5 (2015) 472–480.
- [18] Q. Meng, S. Li, Y. Liu, et al., Circular RNA circSCAF11 accelerates the glioma tumorigenesis through the miR-421/SP1/VEGFA Axis, *Mol. Ther. Nucleic Acids* 17 (2019) 669–677.
- [19] Y. Luo, Y. Fu, R. Huang, et al., CircRNA_101505 sensitizes hepatocellular carcinoma cells to cisplatin by sponging miR-103 and promotes oxidoredo-nitro domain-containing protein 1 expression, *Cell Death Discov.* 5 (2019) 121.
- [20] G. Li, H. Yang, K. Han, et al., A novel circular RNA, hsa_circ_0046701, promotes carcinogenesis by increasing the expression of miR-142-3p target ITGB8 in glioma, *Biochem. Biophys. Res. Commun.* 498 (2018) 254–261.
- [21] G. Yang, T. Zhang, J. Ye, et al., Circ-ITGA7 sponges miR-3187-3p to upregulate ASXL1, suppressing colorectal cancer proliferation, *Cancer Manag. Res.* 11 (2019) 6499–6509.
- [22] Y. Pan, T. Xu, Y. Liu, et al., Upregulated circular RNA circ_0025033 promotes papillary thyroid cancer cell proliferation and invasion via sponging miR-1231 and miR-1304, *Biochem. Biophys. Res. Commun.* 510 (2019) 334–338.
- [23] G. Liu, H. Shi, L. Deng, et al., Circular RNA circ-FOXM1 facilitates cell progression as ceRNA to target PDPF and MACC1 by sponging miR-1304-5p in non-small cell lung cancer, *Biochem. Biophys. Res. Commun.* 513 (2019) 207–212.
- [24] M. Wade, Y.C. Li, G.M. Wahl, MDM2, MDMX and p53 in oncogenesis and cancer therapy, *Nat. Rev. Cancer* 13 (2013) 83–96.
- [25] L.T. Vassilev, B.T. Vu, B. Graves, et al., In vivo activation of the p53 pathway by small-molecule antagonists of MDM2, *Science* 303 (2004) 844–848.
- [26] R. Sawada, R. Maehara, T. Oshikiri, et al., MDM2 copy number increase: a poor prognostic, molecular event in esophageal squamous cell carcinoma, *Hum. Pathol.* 89 (2019) 1–9.
- [27] W. Wang, J. Wu, X. Fei, et al., CHD1L promotes cell cycle progression and cell motility by up-regulating MDM2 in breast cancer, *Am. J. Transl. Res.* 11 (2019) 1581–1592.
- [28] Y. Tang, Y. Xuan, G. Qiao, et al., MDM2 promotes epithelial-mesenchymal transition through activation of Smad2/3 signaling pathway in lung adenocarcinoma, *Onco Targets Ther.* 12 (2019) 2247–2258.